

Homology-Based Image Processing for Automatic Classification of Histopathological Images of Lung Tissue

Mizuho Nishio, Mari Nishio, Naoe Jimbo and Kazuaki Nakane

1. A
 $b_0 = 2, b_1 = 1$



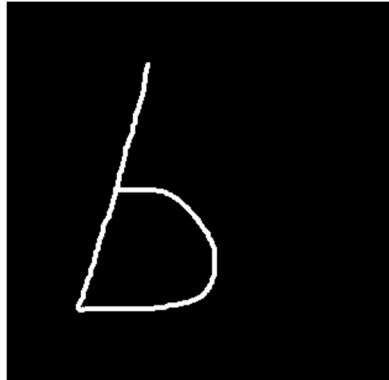
2. a
 $b_0 = 2, b_1 = 1$



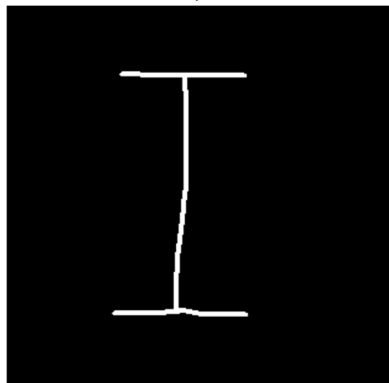
3. B
 $b_0 = 3, b_1 = 1$



4. b
 $b_0 = 2, b_1 = 1$



5. I
 $b_0 = 1, b_1 = 1$



6. i
 $b_0 = 1, b_1 = 2$



Figure S1. Binarized image of handwritten character and its Betti numbers. Note: Betti numbers of binarized image of handwritten character were calculated. In the images, b_0 corresponds to the number of black regions; b_1 corresponds to the number of white regions.

Table S1. Feature names of texture analysis.

Number	Name of Feature
1	original_firstorder_10Percentile
2	original_firstorder_90Percentile
3	original_firstorder_Energy
4	original_firstorder_Entropy
5	original_firstorder_InterquartileRange
6	original_firstorder_Kurtosis
7	original_firstorder_Maximum
8	original_firstorder_MeanAbsoluteDeviation
9	original_firstorder_Mean
10	original_firstorder_Median
11	original_firstorder_Minimum
12	original_firstorder_Range
13	original_firstorder_RobustMeanAbsoluteDeviation
14	original_firstorder_RootMeanSquared
15	original_firstorder_Skewness
16	original_firstorder_TotalEnergy
17	original_firstorder_Uniformity
18	original_firstorder_Variance
19	original_glcM_Autocorrelation
20	original_glcM_ClusterProminence
21	original_glcM_ClusterShade
22	original_glcM_ClusterTendency
23	original_glcM_Contrast
24	original_glcM_Correlation
25	original_glcM_DifferenceAverage
26	original_glcM_DifferenceEntropy
27	original_glcM_DifferenceVariance
28	original_glcM_Id
29	original_glcM_Idm
30	original_glcM_Idmn
31	original_glcM_Idn
32	original_glcM_Imc1
33	original_glcM_Imc2
34	original_glcM_InverseVariance
35	original_glcM_JointEnergy
36	original_glcM_JointEntropy
37	original_glcM_MCC
38	original_glcM_MaximumProbability
39	original_glcM_SumAverage
40	original_glcM_SumEntropy
41	original_glcM_SumSquares
42	original_glrlm_ShortRunEmphasis
43	original_glrlm_LongRunEmphasis
44	original_glrlm_GrayLevelNonUniformity
45	original_glrlm_GrayLevelNonUniformityNormalized
46	original_glrlm_RunLengthNonUniformity
47	original_glrlm_RunLengthNonUniformityNormalized
48	original_glrlm_RunPercentage
49	original_glrlm_GrayLevelVariance
50	original_glrlm_RunVariance
51	original_glrlm_RunEntropy
52	original_glrlm_LowGrayLevelRunEmphasis
53	original_glrlm_HighGrayLevelRunEmphasis
54	original_glrlm_ShortRunLowGrayLevelEmphasis
55	original_glrlm_ShortRunHighGrayLevelEmphasis
56	original_glrlm_LongRunLowGrayLevelEmphasis

57 original_glrlm_LongRunHighGrayLevelEmphasis
58 original_glszm_SmallAreaEmphasis
59 original_glszm_LargeAreaEmphasis
60 original_glszm_GrayLevelNonUniformity
61 original_glszm_GrayLevelNonUniformityNormalized
62 original_glszm_SizeZoneNonUniformity
63 original_glszm_SizeZoneNonUniformityNormalized
64 original_glszm_ZonePercentage
65 original_glszm_GrayLevelVariance
66 original_glszm_ZoneVariance
67 original_glszm_ZoneEntropy
68 original_glszm_LowGrayLevelZoneEmphasis
69 original_glszm_HighGrayLevelZoneEmphasis
70 original_glszm_SmallAreaLowGrayLevelEmphasis
71 original_glszm_SmallAreaHighGrayLevelEmphasis
72 original_glszm_LargeAreaLowGrayLevelEmphasis
73 original_glszm_LargeAreaHighGrayLevelEmphasis
74 original_gldm_SmallDependenceEmphasis
75 original_gldm_LargeDependenceEmphasis
76 original_gldm_GrayLevelNonUniformity
77 original_gldm_DependenceNonUniformity
78 original_gldm_DependenceNonUniformityNormalized
79 original_gldm_GrayLevelVariance
80 original_gldm_DependenceVariance
81 original_gldm_DependenceEntropy
82 original_gldm_LowGrayLevelEmphasis
83 original_gldm_HighGrayLevelEmphasis
84 original_gldm_SmallDependenceLowGrayLevelEmphasis
85 original_gldm_SmallDependenceHighGrayLevelEmphasis
86 original_gldm_LargeDependenceLowGrayLevelEmphasis
87 original_gldm_LargeDependenceHighGrayLevelEmphasis
88 original_ngtdm_Coarseness
89 original_ngtdm_Contrast
90 original_ngtdm_Busyness
91 original_ngtdm_Complexity
92 original_ngtdm_Strength

Table S2. Validation accuracies of CAD with homology-based image processing in the private dataset.

Normalization	Feature Selection	Image Resolutions			Five-Category Accuracy	Optimal Machine Learning Algorithm	
0	0	128 × 128			0.85	1	
0	0	256 × 256			0.795	6	
0	0	256 × 256	128 × 128		0.835	6	
0	0	512 × 512			0.84	7	
0	0	512 × 512	128 × 128		0.84	7	
0	0	512 × 512	256 × 256		0.84	7	
0	0	512 × 512	256 × 256	128 × 128	0.86	7	
0	0	1024 × 1024			0.645	5	
0	0	1024 × 1024	128 × 128		0.695	6	
0	0	1024 × 1024	256 × 256		0.735	6	
0	0	1024 × 1024	256 × 256	128 × 128	0.765	7	
0	0	1024 × 1024	512 × 512		0.73	6	
0	0	1024 × 1024	512 × 512	128 × 128	0.755	7	
0	0	1024 × 1024	512 × 512	256 × 256	0.76	6	
0	0	1024 × 1024	512 × 512	256 × 256	128 × 128	0.77	7
0	1	128 × 128			0.81	1	
0	1	256 × 256			0.9	6	
0	1	256 × 256	128 × 128		0.845	6	
0	1	512 × 512			0.8	7	
0	1	512 × 512	128 × 128		0.865	7	
0	1	512 × 512	256 × 256		0.84	6	
0	1	512 × 512	256 × 256	128 × 128	0.835	7	
0	1	1024 × 1024			0.685	6	
0	1	1024 × 1024	128 × 128		0.795	6	
0	1	1024 × 1024	256 × 256		0.795	6	
0	1	1024 × 1024	256 × 256	128 × 128	0.81	6	
0	1	1024 × 1024	512 × 512		0.785	6	
0	1	1024 × 1024	512 × 512	128 × 128	0.805	6	
0	1	1024 × 1024	512 × 512	256 × 256	0.805	6	
0	1	1024 × 1024	512 × 512	256 × 256	128 × 128	0.815	6
1	0	128 × 128			0.77	6	
1	0	256 × 256			0.795	6	
1	0	256 × 256	128 × 128		0.84	6	
1	0	512 × 512			0.84	7	
1	0	512 × 512	128 × 128		0.84	7	
1	0	512 × 512	256 × 256		0.84	7	
1	0	512 × 512	256 × 256	128 × 128	0.86	7	
1	0	1024 × 1024			0.66	1	
1	0	1024 × 1024	128 × 128		0.705	1	
1	0	1024 × 1024	256 × 256		0.76	3	
1	0	1024 × 1024	256 × 256	128 × 128	0.765	7	
1	0	1024 × 1024	512 × 512		0.73	6	
1	0	1024 × 1024	512 × 512	128 × 128	0.755	7	
1	0	1024 × 1024	512 × 512	256 × 256	0.76	0	
1	0	1024 × 1024	512 × 512	256 × 256	128 × 128	0.775	0
1	1	128 × 128			0.82	6	
1	1	256 × 256			0.865	6	
1	1	256 × 256	128 × 128		0.88	6	
1	1	512 × 512			0.825	7	
1	1	512 × 512	128 × 128		0.88	7	
1	1	512 × 512	256 × 256		0.885	5	
1	1	512 × 512	256 × 256	128 × 128	0.835	7	
1	1	1024 × 1024			0.665	6	
1	1	1024 × 1024	128 × 128		0.855	6	
1	1	1024 × 1024	256 × 256		0.83	6	
1	1	1024 × 1024	256 × 256	128 × 128	0.8	6	
1	1	1024 × 1024	512 × 512		0.765	6	
1	1	1024 × 1024	512 × 512	128 × 128	0.85	6	
1	1	1024 × 1024	512 × 512	256 × 256	0.86	6	
1	1	1024 × 1024	512 × 512	256 × 256	128 × 128	0.86	6

Table S3. Validation accuracies of CAD with texture analysis in the private dataset.

Normalization	Feature Selection	Image Resolutions			Five-Category Accuracy	Optimal Machine Learning Algorithm	
0	0	128 × 128			0.77	5	
0	0	256 × 256			0.715	6	
0	0	256 × 256	128 × 128		0.72	7	
0	0	512 × 512			0.705	5	
0	0	512 × 512	128 × 128		0.695	6	
0	0	512 × 512	256 × 256		0.715	5	
0	0	512 × 512	256 × 256	128 × 128	0.71	5	
0	0	1024 × 1024			0.72	6	
0	0	1024 × 1024	128 × 128		0.815	5	
0	0	1024 × 1024	256 × 256		0.655	6	
0	0	1024 × 1024	256 × 256	128 × 128	0.74	5	
0	0	1024 × 1024	512 × 512		0.65	5	
0	0	1024 × 1024	512 × 512	128 × 128	0.725	6	
0	0	1024 × 1024	512 × 512	256 × 256	0.69	6	
0	0	1024 × 1024	512 × 512	256 × 256	128 × 128	0.665	5
0	1	128 × 128			0.73	5	
0	1	256 × 256			0.81	2	
0	1	256 × 256	128 × 128		0.75	6	
0	1	512 × 512			0.835	2	
0	1	512 × 512	128 × 128		0.725	6	
0	1	512 × 512	256 × 256		0.85	2	
0	1	512 × 512	256 × 256	128 × 128	0.725	6	
0	1	1024 × 1024			0.865	1	
0	1	1024 × 1024	128 × 128		0.755	6	
0	1	1024 × 1024	256 × 256		0.745	6	
0	1	1024 × 1024	256 × 256	128 × 128	0.735	6	
0	1	1024 × 1024	512 × 512		0.71	6	
0	1	1024 × 1024	512 × 512	128 × 128	0.7	6	
0	1	1024 × 1024	512 × 512	256 × 256	0.73	5	
0	1	1024 × 1024	512 × 512	256 × 256	128 × 128	0.74	6
1	0	128 × 128			0.83	3	
1	0	256 × 256			0.77	3	
1	0	256 × 256	128 × 128		0.78	4	
1	0	512 × 512			0.8	0	
1	0	512 × 512	128 × 128		0.815	4	
1	0	512 × 512	256 × 256		0.77	3	
1	0	512 × 512	256 × 256	128 × 128	0.8	4	
1	0	1024 × 1024			0.77	4	
1	0	1024 × 1024	128 × 128		0.815	5	
1	0	1024 × 1024	256 × 256		0.815	2	
1	0	1024 × 1024	256 × 256	128 × 128	0.81	4	
1	0	1024 × 1024	512 × 512		0.805	1	
1	0	1024 × 1024	512 × 512	128 × 128	0.82	3	
1	0	1024 × 1024	512 × 512	256 × 256	0.835	3	
1	0	1024 × 1024	512 × 512	256 × 256	128 × 128	0.825	4
1	1	128 × 128			0.825	0	
1	1	256 × 256			0.81	6	
1	1	256 × 256	128 × 128		0.83	4	
1	1	512 × 512			0.8	4	
1	1	512 × 512	128 × 128		0.8	0	
1	1	512 × 512	256 × 256		0.795	4	
1	1	512 × 512	256 × 256	128 × 128	0.8	4	
1	1	1024 × 1024			0.72	2	
1	1	1024 × 1024	128 × 128		0.82	4	
1	1	1024 × 1024	256 × 256		0.82	4	
1	1	1024 × 1024	256 × 256	128 × 128	0.82	4	
1	1	1024 × 1024	512 × 512		0.79	4	
1	1	1024 × 1024	512 × 512	128 × 128	0.8	4	
1	1	1024 × 1024	512 × 512	256 × 256	0.82	3	
1	1	1024 × 1024	512 × 512	256 × 256	128 × 128	0.815	4

Table S4. Validation accuracies of CAD with homology-based image processing in the public dataset.

Normalization	Feature Selection	Image Resolutions			Three-Category Accuracy	Optimal Machine Learning Algorithm	
0	0	96 × 96			0.9810	7	
0	0	192 × 192			0.9907	7	
0	0	192 × 192	96 × 96		0.9913	7	
0	0	384 × 384			0.9923	7	
0	0	384 × 384	96 × 96		0.9923	7	
0	0	384 × 384	192 × 192		0.9917	7	
0	0	384 × 384	192 × 192	96 × 96	0.9927	7	
0	0	768 × 768			0.9897	7	
0	0	768 × 768	96 × 96		0.9910	7	
0	0	768 × 768	192 × 192		0.9900	7	
0	0	768 × 768	192 × 192	96 × 96	0.9913	7	
0	0	768 × 768	384 × 384		0.9927	7	
0	0	768 × 768	384 × 384	96 × 96	0.9907	7	
0	0	768 × 768	384 × 384	192 × 192	0.9900	7	
0	0	768 × 768	384 × 384	192 × 192	96 × 96	0.9927	7
0	1	96 × 96			0.9250	7	
0	1	192 × 192			0.9633	7	
0	1	192 × 192	96 × 96		0.9740	7	
0	1	384 × 384			0.9710	7	
0	1	384 × 384	96 × 96		0.9827	7	
0	1	384 × 384	192 × 192		0.9740	7	
0	1	384 × 384	192 × 192	96 × 96	0.9807	7	
0	1	768 × 768			0.9687	7	
0	1	768 × 768	96 × 96		0.9793	7	
0	1	768 × 768	192 × 192		0.9783	7	
0	1	768 × 768	192 × 192	96 × 96	0.9810	7	
0	1	768 × 768	384 × 384		0.9773	7	
0	1	768 × 768	384 × 384	96 × 96	0.9833	7	
0	1	768 × 768	384 × 384	192 × 192	0.9820	7	
0	1	768 × 768	384 × 384	192 × 192	96 × 96	0.9847	7
1	0	96 × 96			0.9810	7	
1	0	192 × 192			0.9907	7	
1	0	192 × 192	96 × 96		0.9913	7	
1	0	384 × 384			0.9923	7	
1	0	384 × 384	96 × 96		0.9923	7	
1	0	384 × 384	192 × 192		0.9917	7	
1	0	384 × 384	192 × 192	96 × 96	0.9927	7	
1	0	768 × 768			0.9897	7	
1	0	768 × 768	96 × 96		0.9910	7	
1	0	768 × 768	192 × 192		0.9903	2	
1	0	768 × 768	192 × 192	96 × 96	0.9913	7	
1	0	768 × 768	384 × 384		0.9927	7	
1	0	768 × 768	384 × 384	96 × 96	0.9907	7	
1	0	768 × 768	384 × 384	192 × 192	0.9927	2	
1	0	768 × 768	384 × 384	192 × 192	96 × 96	0.9927	7
1	1	96 × 96			0.9307	7	
1	1	192 × 192			0.9647	7	
1	1	192 × 192	96 × 96		0.9700	7	
1	1	384 × 384			0.9700	7	
1	1	384 × 384	96 × 96		0.9813	7	
1	1	384 × 384	192 × 192		0.9750	7	
1	1	384 × 384	192 × 192	96 × 96	0.9813	7	
1	1	768 × 768			0.9697	7	
1	1	768 × 768	96 × 96		0.9810	7	
1	1	768 × 768	192 × 192		0.9787	7	
1	1	768 × 768	192 × 192	96 × 96	0.9810	7	
1	1	768 × 768	384 × 384		0.9747	7	
1	1	768 × 768	384 × 384	96 × 96	0.9850	7	
1	1	768 × 768	384 × 384	192 × 192	0.9823	7	
1	1	768 × 768	384 × 384	192 × 192	96 × 96	0.9850	7

Table S5. Validation accuracies of CAD with texture analysis in the public dataset.

Normalization	Feature Selection	Image Resolutions				Three-Category Accuracy	Optimal Machine Learning Algorithm
0	0	96 × 96				0.9867	7
0	0	192 × 192				0.9873	7
0	0	192 × 192	96 × 96			0.9893	7
0	0	384 × 384				0.9873	7
0	0	384 × 384	96 × 96			0.9897	7
0	0	384 × 384	192 × 192			0.9877	7
0	0	384 × 384	192 × 192	96 × 96		0.9907	7
0	0	768 × 768				0.9873	7
0	0	768 × 768	96 × 96			0.9913	7
0	0	768 × 768	192 × 192			0.9880	7
0	0	768 × 768	192 × 192	96 × 96		0.9890	7
0	0	768 × 768	384 × 384			0.9897	7
0	0	768 × 768	384 × 384	96 × 96		0.9890	7
0	0	768 × 768	384 × 384	192 × 192		0.9877	7
0	0	768 × 768	384 × 384	192 × 192	96 × 96	0.9923	7
0	1	96 × 96				0.9707	7
0	1	192 × 192				0.9767	7
0	1	192 × 192	96 × 96			0.9787	7
0	1	384 × 384				0.9653	7
0	1	384 × 384	96 × 96			0.9763	7
0	1	384 × 384	192 × 192			0.9757	7
0	1	384 × 384	192 × 192	96 × 96		0.9803	7
0	1	768 × 768				0.9650	7
0	1	768 × 768	96 × 96			0.9783	7
0	1	768 × 768	192 × 192			0.9773	7
0	1	768 × 768	192 × 192	96 × 96		0.9803	7
0	1	768 × 768	384 × 384			0.9633	7
0	1	768 × 768	384 × 384	96 × 96		0.9780	7
0	1	768 × 768	384 × 384	192 × 192		0.9777	7
0	1	768 × 768	384 × 384	192 × 192	96 × 96	0.9827	7
1	0	96 × 96				0.9867	7
1	0	192 × 192				0.9873	7
1	0	192 × 192	96 × 96			0.9893	7
1	0	384 × 384				0.9873	7
1	0	384 × 384	96 × 96			0.9897	7
1	0	384 × 384	192 × 192			0.9877	7
1	0	384 × 384	192 × 192	96 × 96		0.9917	7
1	0	768 × 768				0.9873	7
1	0	768 × 768	96 × 96			0.9907	7
1	0	768 × 768	192 × 192			0.9883	7
1	0	768 × 768	192 × 192	96 × 96		0.9890	7
1	0	768 × 768	384 × 384			0.9893	7
1	0	768 × 768	384 × 384	96 × 96		0.9893	7
1	0	768 × 768	384 × 384	192 × 192		0.9880	7
1	0	768 × 768	384 × 384	192 × 192	96 × 96	0.9923	7
1	1	96 × 96				0.9707	7
1	1	192 × 192				0.9767	7
1	1	192 × 192	96 × 96			0.9777	7
1	1	384 × 384				0.9653	7
1	1	384 × 384	96 × 96			0.9767	7
1	1	384 × 384	192 × 192			0.9757	7
1	1	384 × 384	192 × 192	96 × 96		0.9803	7
1	1	768 × 768				0.9643	7
1	1	768 × 768	96 × 96			0.9767	7
1	1	768 × 768	192 × 192			0.9773	7
1	1	768 × 768	192 × 192	96 × 96		0.9810	7
1	1	768 × 768	384 × 384			0.9633	7
1	1	768 × 768	384 × 384	96 × 96		0.9777	7
1	1	768 × 768	384 × 384	192 × 192		0.9777	7
1	1	768 × 768	384 × 384	192 × 192	96 × 96	0.9820	7



© 2021 by the authors. Licensee MDPI, Basel, Switzerland. This article is an open access article distributed under the terms and conditions of the Creative Commons Attribution (CC BY) license (<http://creativecommons.org/licenses/by/4.0/>).